ELSEVIER

Journal of Power Sources 96 (2001) 68–75

JOURNAL OF POWER SOURCES

www.elsevier.com/locate/jpowsour

Nickel metal hydride batteries for high power applications

M. Luisa Soria[a,*], Joaquín Chacón[b], J. Carlos Hernández[b], Daniel Moreno[a], Araceli Ojeda[a]

[a]*Tudor Research Laboratory, Exide Technologies, Ctra. N-II, km 42, E-19200 Azuqueca de Henares, Spain*
[b]*Electro Mercantil Industrial, Exide Technologies, Hierro 38, E-28850 Torrejón de Ardoz, Spain*

Received 1 December 2000; accepted 4 December 2000

Abstract

Nickel metal hydride (Ni/MH) is presently the most promising battery system for electric and hybrid vehicle propulsion in the short and mid-term. This paper presents the results obtained in the development of prismatic Ni/MH batteries for high power, mainly hybrid vehicle, applications.

Valve regulated Ni/MH cells rated at 25 and 60 Ah have been designed and assembled using improved positive and negative electrodes. Both types of cells showed excellent high rate discharge capability and fast rechargeability and a satisfactory charge retention when stored and cycle life under deep cycling and hybrid vehicle working conditions. On the other hand, energy and power efficiency ratios were improved in the 60 Ah cells.

Keywords: Nickel metal hydride batteries; High rate applications; Hybrid vehicles; Electrical testing

1. Introduction

There is a clear need for clean transportation means, specially in the big cities. Air pollution and the ''Green House effect'' are environmental problems that can force European legislation into laws similar to the Californian ''Clean Air Act'' (1988). However, the final acceptance of zero-emission or hybrid vehicles will depend strongly on the final performance of the batteries and on its acquisition price and maintenance costs. Ni/MH is presently the most promising battery system for hybrid vehicle propulsion in the short and mid-term.

During the last decade, the use of Ni/MH batteries [1] has spread quickly for consumer applications, mainly for portable electronic equipment. However, power capability should be improved to answer the increased power demands of the different types of hybrid vehicles (range extender, power assist), and even for the future conventional cars with 42 V electrical systems. The final acceptance of hybrid vehicles will depend on the performance/cost ratio achieved. Also in comparison to the outcome of competing technologies for low and zero-emission vehicles, including the efforts to reduce emissions in conventional gasoline combustion engines and the development of low emission vehicles using alternative fuels such as natural gas.

This paper presents the results obtained in the development of Ni/MH batteries for high power applications, mainly hybrid vehicles. The work was carried out within a EU funded project [2] aimed at the development of positive electrodes using a novel type of nickel hydroxide characterised by an irregular shaped grain structure and a high tap density.

2. Experimental

The development of the positive and negative electrodes for Ni/MH batteries has been reported previously [3,4]. Both types of electrodes were prepared with three dimensional nickel substrates in order to improve the high power capability of the electrodes by means of the conductive network and with additives to decrease the electrode internal resistance.

The nickel hydroxide doped with cobalt and zinc was provided by R.B.C. and was prepared according to a novel electrodialysis process [5], followed by ageing in a KOH solution to promote the β-phase and increase crystallinity. This material is characterised by a high tap density, an irregular shape and a high BET surface area (35–40 $m^2\ g^{-1}$). It has been described as a highly defective

* Corresponding author. Tel.: +34-949-263-316; fax: +34-949-262-560.
E-mail address: soriaml@tudor.es (M.L. Soria).

0378-7753/01/$ – see front matter
PII: S0378-7753(00)00677-7

Table 1
Characteristics of optimised positive and negative electrodes

	Positive electrodes	Negative electrodes
Substrate type	Ni foam	Ni fibre
Weight (g m^{-2})	500	950
Electroactive material	$Ni(OH)_2$ doped with Co (1.5%) and Zn (3.5%)	LaMM($Ni_{3.4}Mn_{0.4}Al_{0.3}Co_{0.7}$) 52% La in MM
Additives (%)	Ni powder (15) Co + CoO (5) PTFE (3) Arabic gum (0.7)	Extra-conductive black (3.2) PTFE (1.6) PVA (0.2)
Preparation conditions	Pasting + pressing	Rolling + pressing

material, a fact that is associated with a complex electrochemical behaviour [6,7]. Doping with cobalt and zinc improves the active material efficiency, cycleability and high temperature performance [8,9].

The AB_5 alloy used for the negative electrodes was supplied by GfE Metalle und Materialien with the standard composition LaMM($Ni_{3.4}Mn_{0.4}Al_{0.3}Co_{0.7}$) (MM: misch metal) [10]. A mechanical treatment of the alloy was provided by the manufacturer to improve the material power capability [11].

Different additives were used with the aim of improving the performance of the active materials, in terms of conductivity, adequate rheological properties for electrode preparation and to avoid the active material shedding during cycling. The positive and negative electrode preparation conditions were finally optimised according to the materials used and the high power demanding application. Table 1 summarises the characteristics and composition of both types of electrodes.

As shown in the table, the positive active material [12,13] included nickel powder and cobalt compounds to increase conductivity, natural or synthetic polysaccharides to adjust paste rheology thus improving processing conditions and polytetrafluorethylene (PTFE) as binder of the particles, to avoid active material shedding during battery manufacturing and operation. In the negative electrodes, extra-conductive blacks were used to increase conductivity and PTFE and PVA as binders [14–16].

Table 2 shows the capacity ratios of the optimised electrodes used in the assembly of Ni/MH prismatic cells.

Table 2
Capacity ratios of the optimised positive and negative electrodes

	Positive electrodes	Negative electrodes
Capacity *C*/5 rate		
mAh g^{-1} active material	275	278
mAh g^{-1} electrode	157	179
mAh cm^{-3} electrode	340	677
Capacity 7*C* rate		
mAh g^{-1} active material	132	180
mAh g^{-1} electrode	75	116
mAh cm^{-3} electrode	164	435

Two types of Ni/MH prismatic cells with stacked electrodes have been assembled, with a nominal capacity of 25 and 60 Ah, respectively. Table 3 shows the main features of both types of cells.

All the cell components have been specially designed to achieve the maximum power drain (minimum electrical resistance), with minimum weight and a valve regulated maintenance-free system. Besides the electrodes, the separator and the valve have been studied as key components of the cell to achieve the improved performance and maintenance-free operation. A solution of KOH, 1.30 g cm^{-3} with 20 g l^{-1} LiOH, was used as electrolyte in the cells, impregnating the electrodes and separator. The incorporation of lithium ions in the nickel lattice combined with the co-deposited cobalt, enhances the charge acceptance of the positive electrodes, specially at elevated temperatures, due to the stabilisation of high oxidation states [17].

Table 3
Ni/MH cell design features and components

Nominal capacity (Ah)	25	60
Cell dimensions (mm^3)	80 × 34 × 133	114 × 45 × 158
Plate number (±)	12/11	15/14
Plate dimensions (mm^2)	90 × 70	110 × 105
Separator	SciMAT 700/14 (grafted polyolefine)	SciMAT 700/14 (grafted polyolefine)
Electrolyte	KOH 1.3 g cm^{-3} + LiOH 20 g l^{-1}	KOH 1.3 g cm^{-3} + LiOH 20 g l^{-1}
Case and cover	Stainless steel, 0.4 mm thick	Stainless steel, 0.4 mm thick
Cell weight (kg)	0.89	1.95

Table 4
Electrical testing programme of Ni/MH cells

	Testing conditions
Constant current discharges at different rates	Discharge at the xC rate, being $x = 0.2, 0.5, 1, \ldots, 10$ at room temperature
Constant current discharges at different temperatures	Discharge at the 1C rate at room temperature: 0 and 40°C
Power capability	Discharge during 10 s at the 10C rate and at different states of charge: 100, 80, 60, 40 and 20% SOC
Constant current charging at different rates	Charge at the yC rate, being $y = 0.2, 0.5, \ldots, 4$, with a charge factor of 120% at room temperature
Charging efficiency for different states of charge	Recharge the cells at the 1C rate with recharge factors between 50 and 120%
Rapid charge capability	Discharge at the C/2 rate down to 40% SOC Recharge between 40 and 80% SOC at the 2C, 5C and 8C rates
Self-discharge	Capacity retention after 48 and 120 h storage at room temperature and 40°C and after 28 days storage at room temperature
Cycle life	Constant current conditions at the C/5 and 1C rates (100% DOD) and according to EUCAR power assist profile
Recombination efficiency	Weight loss during cell overcharge at the C/20 rate

The separator must be characterised by a low internal resistance, to achieve high rate performance (related to thickness and porosity), small pores to avoid short-circuits, high electrolyte absorption, good wettability and chemical stability in alkaline electrolyte even at high temperature. On the other hand, polypropylene non-woven materials grafted with acrylic monomers show enough wettability and ionic exchange capability during battery operation [18].

Valves are quite important elements of the cells, as the internal pressure can rise during overcharge. The functions of the valve are to protect the cell from entering oxygen, to keep H_2 gas in the cell (lower water consumption) and to ensure opening as soon as the internal pressure limit is reached. The valve is designed according to the pressure evolution inside the cell during charge and discharge conditions.

Electrical testing of the Ni/MH cells has been carried out with a computer-controlled cycling equipment (Bitrode LCN-3-100-12) with modules CSM-6-100-12 for testing individual cells. High rate battery discharges have been performed with a Digatron UBT, BTS-500, model HEW 2000-6BTS. Data acquisition was performed with the software available (Bitrode and Digatron) and with a data logger Datataker 505. Temperature measurements were carried out with thermocouples type J.

After cell formation and initial cycling at the C/5 rate (C being the rated capacity of 25 or 60 Ah), the Ni/MH cells were tested according to the conditions mentioned in Table 4.

3. Results and discussion

Battery testing conditions were defined according to the nominal capacity of the cells, i.e. 25 and 60 Ah. Previous to all the discharge tests, the cells were charged during 7 h at the C/5 rate. Discharged capacities depend on the testing rates and, at low rates (C/5), the figures obtained are around 110–115% of the nominal capacity.

Figs. 1 and 2 show the constant current discharge curves at different rates, respectively. The results are referred to the nominal capacity (25 or 60 Ah) of the cells. The maximum battery capacity values obtained were 28.9 and 69.2 Ah at the C/5 rate. After each discharge at the xC rate, the cells were further discharged at the C/5 rate down to 1.0 V. As shown in the figures, discharge duration depends mainly on the discharge voltage, that means, on the internal resistance of the cell. At the 8C rate, 73% of the real capacity, i.e. 84% of the nominal capacity, is obtained when the 25 Ah cells are discharged down to 0.8 V. The cells rated at 60 Ah deliver 56% of the nominal capacity when discharged at the 10C rate down to 0.6 V. The cell temperature has been measured during the discharges: the 60 Ah cells showed a temperature increases of 6, 10, 14 and 20°C during the discharges at 120, 240, 420 and 600 A, respectively. Heating is mainly due to Joule effect ascribed to the internal resistance of the cells. The metallic container allows for an efficient heat dissipation.

The internal resistance of the cells has been measured both under AC (1 kHz) and DC conditions. The AC resistance of the Ni/MH batteries is 1.6 mΩ for the 25 Ah cells and 1.2 mΩ for the 60 Ah cells. The DC resistance has been calculated taking into account the voltage drop of the cells when discharged at two different rates: 1C and 8C for the 25 Ah cells and 1C and 10C for the 60 Ah cells. The values obtained are 1.67 and 1.24 mΩ, respectively.

In order to establish the temperature influence on the discharge duration, the 60 Ah Ni/MH cells were discharged at 60 A (1C rate) after 18 h storage at three different temperatures: 0, 25 (room temperature) and 40°C. Referred to the capacity obtained at room temperature, the cells showed a 9% decrease in battery capacity at 0°C and a 10% decrease at 40°C.

The power capability of the Ni/MH cells was tested at different SOC: the 60 Ah cells were discharged according to a sequence of current peaks at 600 A at the 100, 80, 60, 40 and 20% SOC, followed by a discharge at 12 A (C/5 rate) to reach the following SOC check point. The discharge curve is represented in Fig. 3. On the other hand, Fig. 4 shows the power values calculated at the different SOC.

Moreover, the AC internal resistance of the Ni/MH cells at the different states of charge has been measured. The values

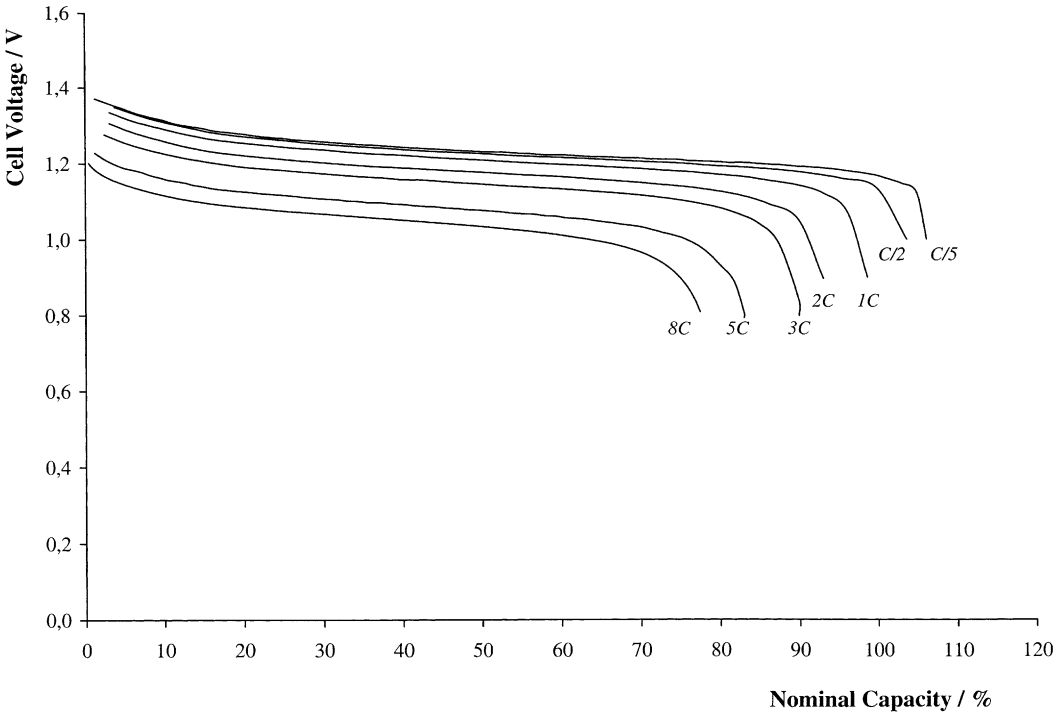

Fig. 1. Constant discharge curves at different rates of Ni/MH cells ($C = 25$ Ah).

recorded indicate that there is no significant effect of the SOC on the internal resistance as it increased 0.03 mΩ during the discharge.

The rechargeability test included constant current charges at $C/5$, $C/2$, $1C$, $2C$ and $4C$, and the recharge factor was $1.2C$ in all cases. After each charge, the cells were discharged at the $C/5$ rate down to 1.0 V. Fig. 5 shows the charge curves of the cells rated 25 Ah. The 60 Ah cells showed similar charging curves. The temperature increase during the charges of the 60 Ah cells was 5, 8, 10, 13 and

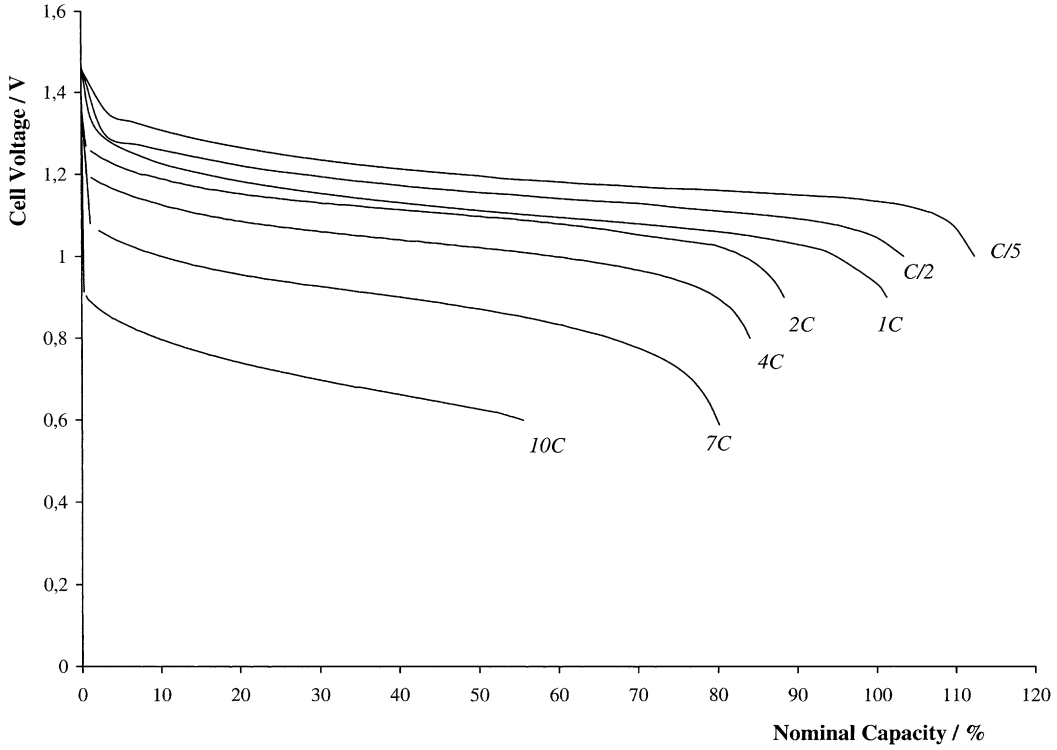

Fig. 2. Constant discharge curves at different rates of Ni/MH cells ($C = 60$ Ah).

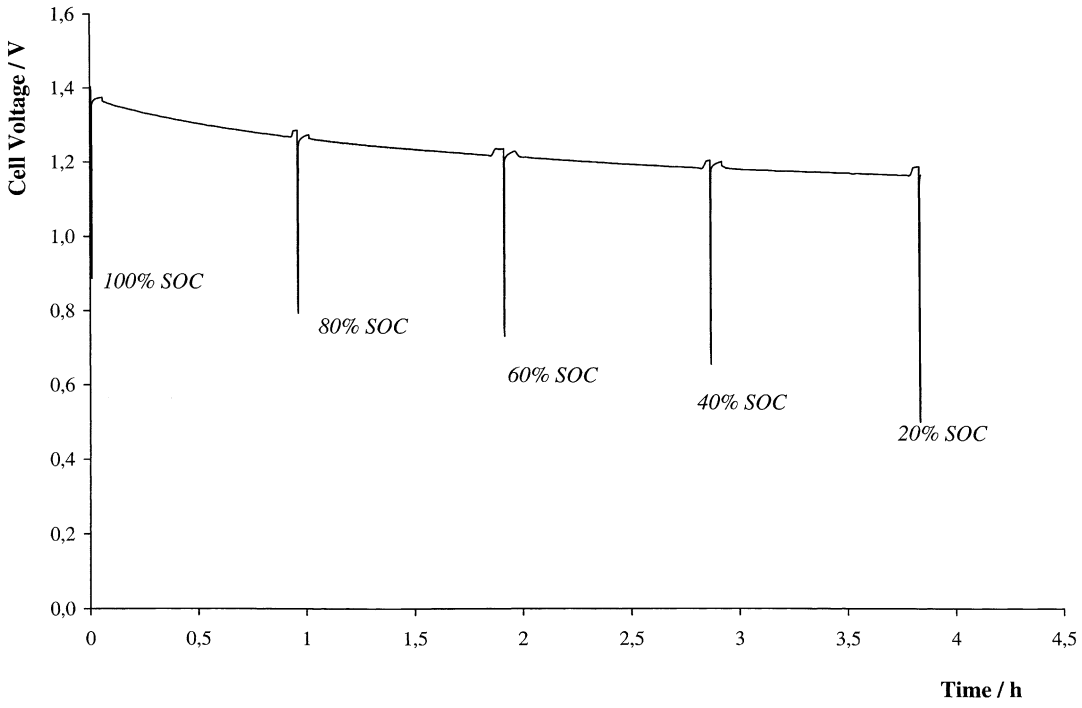

Fig. 3. Power capability discharge test of Ni/MH cells ($C = 60$ Ah).

25°C for the charges at $C/5$, $C/2$, $1C$, $2C$ and $4C$ rates, respectively.

The discharged capacity (at the $C/5$ rate) obtained after each constant current charge for both types of cells is represented in Fig. 6, where for comparison purposes the capacity at the $C/5$ rate of the cells corresponds to a 100% value, according to the following formula:

$$\text{Discharged capacity}(\%) = \frac{\text{Capacity(Ah) at the } yC \text{ rate}}{\text{Capacity at the } C/5 \text{ rate(Ah)}} \times 100$$

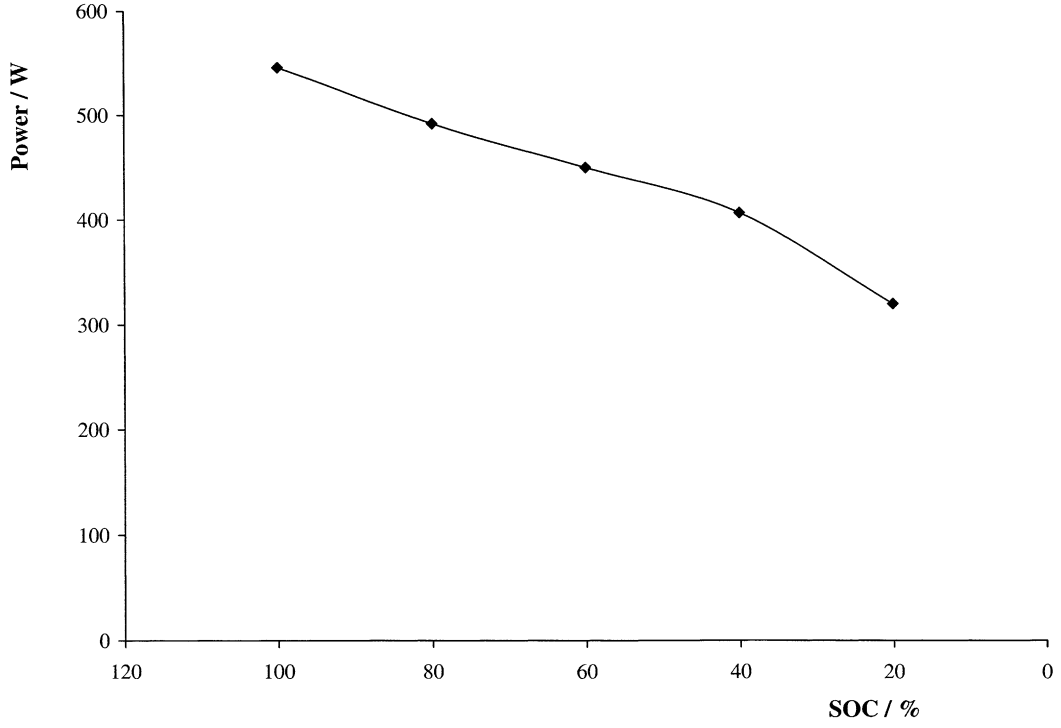

Fig. 4. Power capability of Ni/MH cells at 600 A and at different states of charge ($C = 60$ Ah).

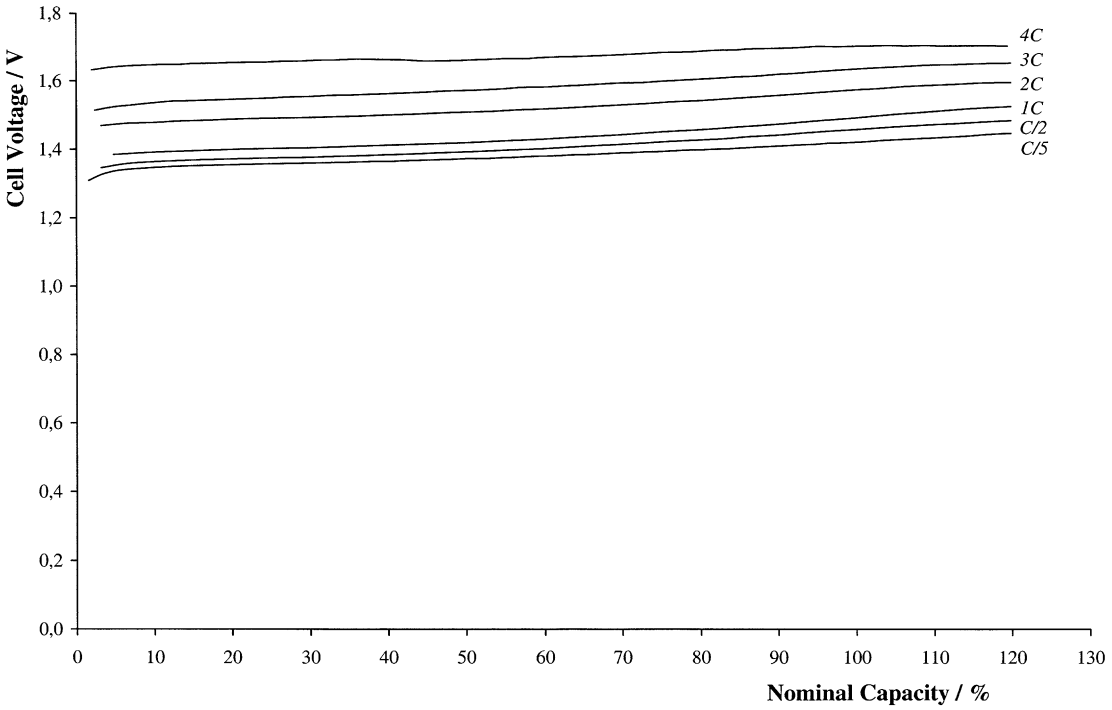

Fig. 5. Constant charge curves at different rates of Ni/MH cells ($C = 25$ Ah).

The figure clearly shows that in both cases the best charging efficiency is obtained when the cells are recharged at the 1*C* rate, and that up to 2*C* rate the values are over 100%.

The charging efficiency for different SOC has also been calculated: charging at the 1*C* rate the previously discharged cells and then discharging at the *C*/5 rate down to 1.0 V. Fig. 7 shows the capacity discharged from the 25 Ah cells, expressed as percentage of the nominal capacity after each partial charge. The charging efficiency obtained for the different charging ratios tested is higher than 95%, and

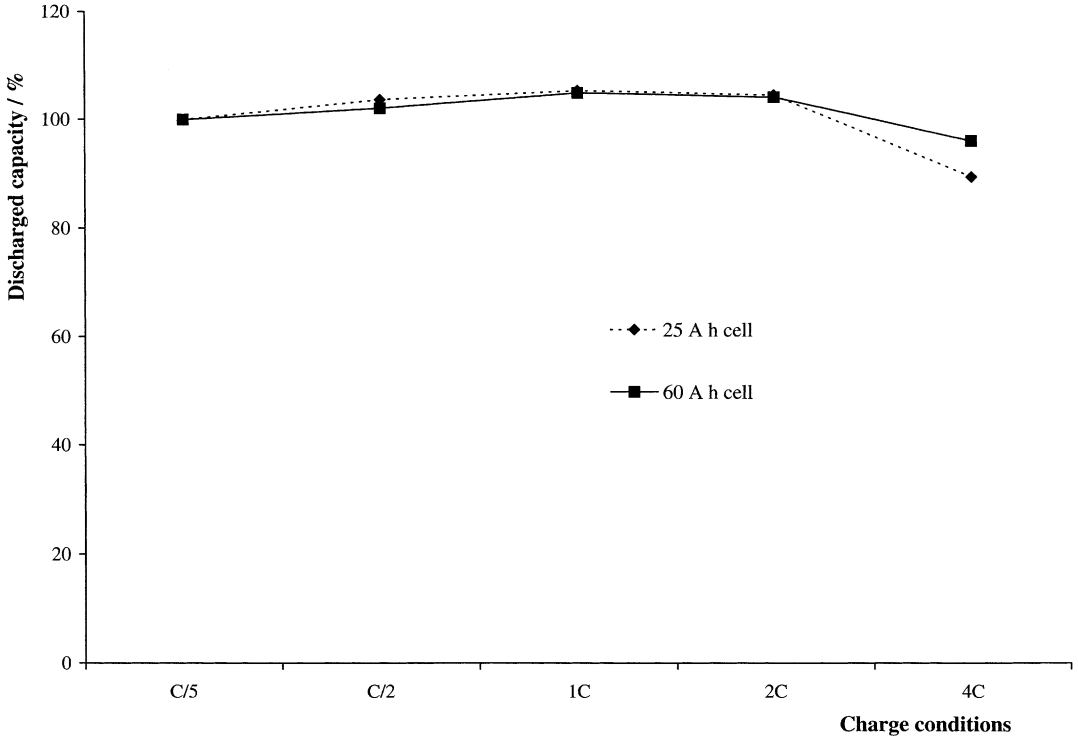

Fig. 6. Discharged capacity after charging at different rates of Ni/MH cells ($C = 25$ and 60 Ah).

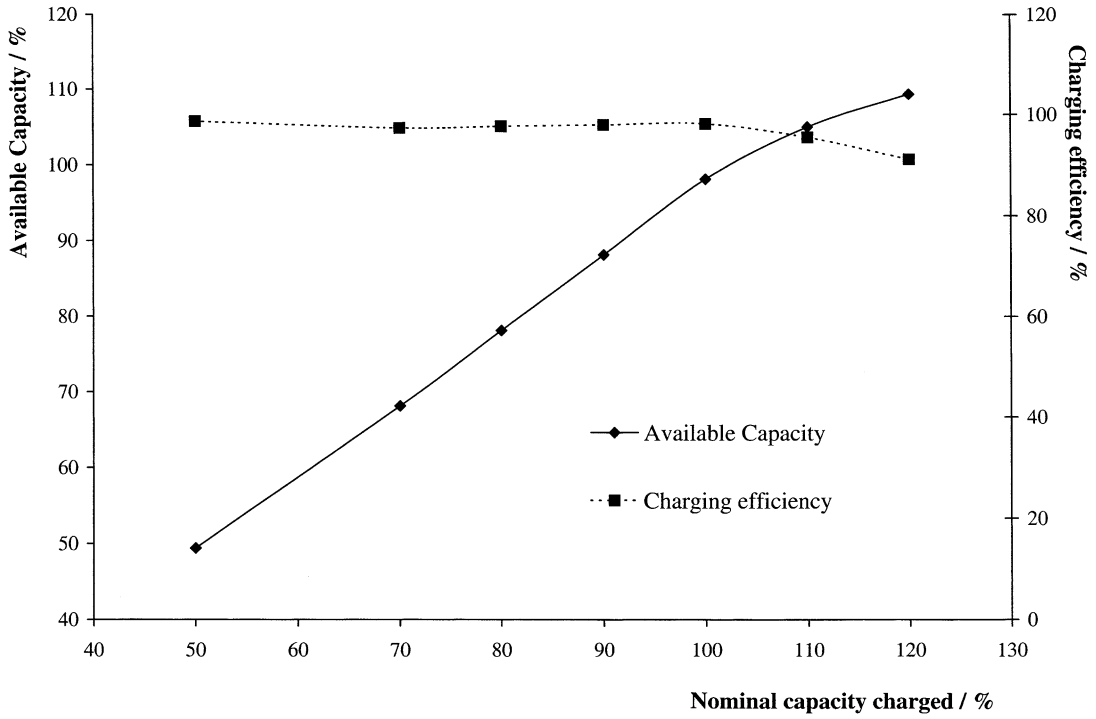

Fig. 7. Charging efficiency of Ni/MH cells at different states of charge ($C = 25$ Ah).

around 97% up to 90% SOC. The 60 Ah cells show a similar behaviour.

On the other hand, the rapid charge capability of the 60 Ah Ni/MH cells has been determined. The test was performed by charging the cells with a high charge current when between 40 and 80% SOC, and calculating, for three different current values, the coulombic and energy efficiency values. Prior to the test, the 60 Ah cells were discharged by 60% of the useful capacity at the *C*/2 rate, i.e. down to 40% SOC. Then they were recharged at 120, 300 and 480 A (2*C*, 5*C* and 8*C* rates, respectively) up to 80% SOC. The discharge duration at the *C*/2 rate to1.0 V was used to calculate the recharge coulombic efficiency, which was higher than 90% for the range 40–80% SOC even at the 8*C* rate. Also the energy efficiency ratios, which ranged between 74% for the 2*C* charge and 61% for the 8*C* charge.

The high efficiency values obtained in the high rate rechargeability tests enable the definition of a quick charge procedure, at least for a few minutes duration and at 80% state of charge, to avoid temperature and internal pressure increases.

The self-discharge test included the measurement of the capacity retained after 48 and 120 h storage at room temperature and at 40°C. The results obtained are satisfactory, as the 60 Ah Ni/MH cells retained 93 and 90% of the initial capacity after 48 and 120 h at room temperature and 90 and 86% after 48 and 120 h at 40°C, respectively. On the other hand, the capacity retained by the 25 Ah cells on storage during 28 days at room temperature was 93% of the initial capacity value.

The cycle life performance of the Ni/MH batteries is being tested, both under constant current conditions at the *C*/2 and 1*C* rates (100% DOD) and in special tests simulating the hybrid vehicle working conditions (power assist profile of the EUCAR specification). To date the results obtained are satisfactory.

Finally, the recombination efficiency of the valve regulated design has been tested by overcharging the Ni/MH cell at the *C*/20 rate after a complete charge. The cell has been weighed periodically, and the weight loss figures have been used to calculate the recombination efficiency, considering that if the current were used for the water electrolysis process, each Ah charged would represent a water consumption of 0.3361 g, according to the following formula:

$$\text{Recombination efficiency}\,(\%) = \left(1 - \frac{\text{Real weight loss}}{\text{Current equivalent water loss}}\right) \times 100$$

Test results show clearly that the recombination efficiency is nearly 100% during the whole test.

4. Conclusions

Valve regulated Ni/MH prismatic cells rated at 25 and 60 Ah have been designed and assembled using high performance electrodes. The cells show excellent high rate discharge capability when on continuous discharges up to the 10*C* rate, due to the high kinetically active materials

and the optimised design of all the components to give a low value of internal resistance.

The high efficiency values obtained in the high rate rechargeability tests enable the definition of fast charge procedures up to 80% SOC without a significant temperature and internal pressure increase. The Ni/MH cells show also a satisfactory performance under deep discharge cycling and when tested to simulate power-assist hybrid vehicle working conditions. The charge retention when stored, even at high temperature, is good. Also, recombination efficiency is nearly 100%, which allows for a maintenance-free operation.

Work performed up to date on the development of prismatic Ni/MH cells for high power applications encourages further studies in order to optimise energy and power battery ratios (Wh kg^{-1} and W kg^{-1}), thus promoting their use for hybrid vehicles and 42 V automotive electrical network systems. However, these applications require the development of battery management systems with algorithms to control continuously the SOC and the state of health (SOH) of the battery. Finally, a battery thermal management can avoid temperature increase during the high rate charging and discharging processes, by means of a forced air draught cooling system.

Acknowledgements

This work has been partially funded by the European Commission within the framework of the Industrial and Materials Technologies Programme (Brite-EuRam Contract BRPR-CT97-0515). The authors wish also to thank the project partners R.B.C. (FR) for the samples of doped nickel hydroxide.

References

[1] J.J.G. Willems, Philips J. Res. 39 (1984) 1.
[2] Brite-EuRam III Project BE97-4219, Contract BRPR-CT97-0515.
[3] M.L. Soria, J. Chacón, J.C. Hernández, in: Proceedings of the International Conference on Advanced Batteries and Accumulators, Brno, CZ, August 2000.
[4] M.L. Soria, J. Chacón, J.C. Hernández, J. Power Sources (2000), submitted for publication.
[5] US Patent 5 384 017 and European Patent 0 559 590.
[6] S. Deabate, F. Fourgeot, F. Henn, J. Power Sources 87 (2000) 125.
[7] S. Deabate, F. Fourgeot, F. Henn, Ionics 5 (1999) 371.
[8] P. Oliva, J. Leonardi, J.F. Laurent, C. Delmas, J.J. Braconnier, M. Figlarz, F. Fievet, A. de Guibert, J. Power Sources 8 (1982) 229.
[9] A.H. Zimmerman, J. Electrochem. Soc. Proc. 94 (27) (1994) 268.
[10] V. Güther, A. Otto, J. Alloys Comp. 293 (1999) 889.
[11] A. Otto, V. Güther, J. Alloys Comp. 293 (1999) 734.
[12] R.D. Armstrong, G.W.D. Briggs, E.A. Charles, J. Appl. Electrochem. 18 (1988) 215.
[13] B. Aladjov, A. Greenberg, S. Gamburzev, W. Zhang, O. Velev, in: Proceedings of the 37th Power Sources Conference, 1996, p. 402.
[14] A. Visintin, D. Smith, M. Gamboa-Aldeco, S. Srinivasan, J. Electrochem. Soc. Proc. 97 (18) (1997) 780.
[15] L. Aymard, C. Lenain, L. Courvoisier, F. Salver-Disma, J.-M. Tarascon, J. Electrochem. Soc. 146 (1999) 2015.
[16] T. Sakai, A. Takagi, N. Kuriyama, H. Miyamura, H. Ishikawa, Prog. Batteries Solar Cells 9 (1990) 269.
[17] A.K. Sood, in: D.A. Corrigan, Nickel Hydroxide Electrodes, Vol. 90–94, The Electrochem. Soc. Inc., Pennington, USA, 1990, p. 163.
[18] J. Cook, Electric and Hybrid Vehicle Tech.'99, 1999, p. 128.